Kinetics of the O + ClO Reaction†

Leah Goldfarb,‡,§ James B. Burkholder, and A. R. Ravishankara*,§

Aeronomy Laboratory, NOAA, 325 Broadway, Boulder, Colorado 80305-3328

Received: January 4, 2001; In Final Form: March 28, 2001

The rate coefficient for the reaction O + ClO → Cl + O_2 (1) was measured over the range 227 to 362 K using a discharge flow tube coupled to a pulsed laser photolysis-atomic resonance fluorescence apparatus. The title reaction was studied under pseudo-first-order conditions in O atoms in an excess of ClO. ClO radicals were produced in the discharge flow tube by the reaction of Cl with either O_3 or Cl_2O and its concentration was measured in situ by UV absorption. O atoms were produced by pulsed laser photolysis of ClO at 308 nm and detected by atomic resonance fluorescence. The measurements yield $k_1(T) = (3.0 \pm 0.8) \times 10^{-11} \exp((75 \pm 40)/T)$ cm^3 molecule^{-1} s^{-1}, where the uncertainties are at the 95% confidence level and include estimated systematic errors. These results are compared with previous data and an expression that can be used for atmospheric purposes is suggested.

Introduction

Chlorine-catalyzed ozone destruction via the reaction mechanism:

$$O + ClO \rightarrow Cl + O_2 \quad (1)$$

$$Cl + O_3 \rightarrow ClO + O_2 \quad (2)$$

$$\text{Net: } O + O_3 \rightarrow 2O_2 \quad (3)$$

plays an important role in determining the abundance of upper stratospheric ozone and its trend over the past two decades.[1] (In this paper, O atom refers to the ground-state oxygen atom, O(^{3}P)). Reaction 1 is the rate-limiting step in this catalytic cycle. Therefore, the rate coefficient, $k_1(T)$, and its temperature dependence, is crucial for calculating ozone levels and its trend. Reaction 1 has been studied numerous times over the past 15 years.[2−8] While there is relatively good agreement among the values of $k_1(T)$ reported in the 1980s, systematic errors in determining the ClO concentration could have affected these investigations. Also, most of these studies used the discharge flow tube method, which constrained the pressures to a few Torr. It is now recognized that ClO can form a dimer at low temperature and more information about the generation of ClO, possible reaction of vibrationally excited ClO with Cl atoms,[9−11] and the absorption cross section of ClO has become available.[12] For stratospheric modeling, the currently recommended[12] value of $k_1(T)$ is $3.0 \times 10^{-11} \exp(70/T)$ cm^3 molecule^{-1} s^{-1}; $k_1(298) = 3.8 \times 10^{-11}$ cm^3 molecule^{-1} s^{-1} and is derived from the studies of the 1980s. Therefore, a careful study of reaction 1 is worthwhile.

We have reinvestigated reaction 1 using an apparatus where a discharge flow tube is coupled to a diode array spectrometer to measure ClO concentration, O atoms are produced via pulsed laser photolysis of ClO, and the temporal profile of O atoms are measured via atomic resonance fluorescence. The rate coefficient for reaction 1, $k_1(T)$, was measured between 227 and 362 K in 2.5 to 18 Torr of N_2.

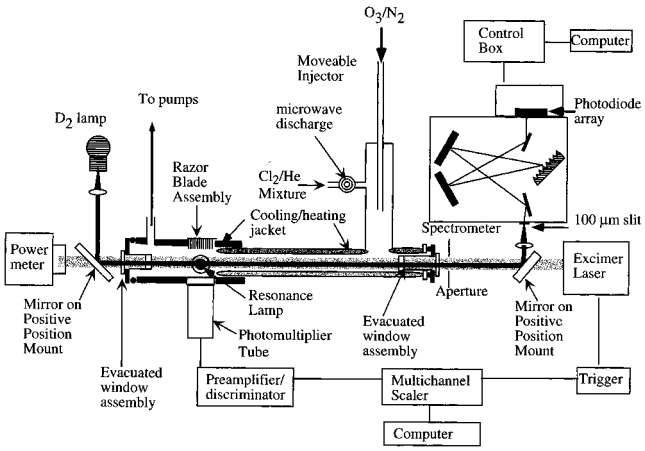

Figure 1. A schematic of the experimental apparatus used to measure k_1. Individual components are noted in the figure and explained in the text.

Experiments

Reaction 1 was studied using a technique that couples a flow tube with a pulsed photolysis system.[11] We have recently used such a system to study the reactions of ClO with OH[10] and IO[11] under pseudo-first-order conditions in OH and IO; these radicals were monitored via laser-induced fluorescence. In this study, we used atomic resonance fluorescence detection of O atoms in an excess of ClO for measuring k_1. This combination of a flow tube and a pulsed photolysis method is described in detail elsewhere.[10,11,13]

The apparatus used to measure k_1 is shown in Figure 1. There are four major components in this apparatus: (1) a flow tube where ClO radicals were generated, (2) an absorption cell where the concentration of ClO was measured, (3) a D_2 lamp (30 W) and a 0.28-m spectrograph equipped with a diode array detector

* Author to whom correspondence should be addressed at NOAA, R/AL2, 325 Broadway, Boulder, CO 80305-3328. E-mail: ravi@al.noaa.gov.

† This work was part of a Ph.D. thesis submitted by L. Goldfarb to the University of Colorado, Boulder, Colorado.

‡ Presently at CNRS/SA, BP N° 3, 91371 Verrières-le-Buisson Cedex, France.

§ Also affiliated with the Department of Chemistry and Biochemistry, University of Colorado, Boulder, CO 80309.

10.1021/jp0100351 CCC: $20.00
Published on Web 05/12/2001

to measure the concentration of ClO (as well as that of O_3, Cl_2O, and Cl_2), and (4) an aluminum reactor, where O atoms were created by 308 nm (XeCl excimer) pulsed laser photolysis of ClO and detected by atomic resonance fluorescence. The individual components have been used in our laboratory extensively.[11,14,15] Therefore, we will describe here only the parts essential for an understanding of this study.

This apparatus differs from the previous flow tube-pulsed photolysis system that was used in the studies of OH + ClO[10] and IO + ClO[11] reactions in a few ways. First, we used an atomic resonance fluorescence cell for the detection of O atoms. Second, the pulsed photolysis-resonance fluorescence detection component was at the end, as opposed to the middle, of the absorption cell; however, it was also a part of the absorption path. Third, the absorption cell and reactor were at the same temperature.

ClO Generation. ClO radicals were produced at 298 K via the reaction of Cl atoms with O_3 or Cl_2O:

$$Cl + O_3 \rightarrow O_2 + ClO \quad (2)$$

or

$$Cl + Cl_2O \rightarrow Cl_2 + ClO \quad (4)$$

where $k_2(298\ K) = 1.2 \times 10^{-11}$ cm^3 molecule^{-1} s^{-1} and $k_4(298\ K) = 9.6 \times 10^{-11}$ cm^3 molecule^{-1} s^{-1}.[12] Cl atoms were produced in a microwave discharge of a Cl_2/He mixture in a sidearm of the discharge flow tube. The concentration of Cl atoms was in large excess over the initial concentration of O_3 or Cl_2O such that reaction 2 or 4 was essentially complete (>99%) in the flow tube. Thus, all the O_3 or Cl_2O was consumed before the flow entered the absorption cell. The absence of O_3 or Cl_2O was verified by measuring the absorption spectra of the gas mixture flowing through the absorption cell.

A mixture of O_3 or Cl_2O in N_2 was added through a movable injector (4 mm i.d.) centered in the flow tube. An additional flow of N_2 (~16 STP cm^3 s^{-1}) was added to this flow to bring the pressure in the flow tube to the desired value of 2.5 to 18 Torr. The amount of He from the Cl_2/He mixture in the flow tube was usually less than ~20% of the total flow; at the lower pressures (i.e., less than ~7 Torr) it constituted a larger fraction. The Cl_2 concentration was $\sim 1 \times 10^{16}$ molecule cm^{-3}. The reaction region of the discharge flow tube (for reactions 2 and 4) was 35 cm long (i.d. = 3 cm). The linear gas flow velocity in this region was roughly 400−700 cm s^{-1}. The Cl atom concentration in the flow tube was greater than $\sim 2 \times 10^{14}$ atom cm^{-3}. Therefore, the time for conversion of O_3 or Cl_2O to ClO in the flow tube was 50−85 ms, in which time reactions 2 and 4 essentially went to completion and consumed all O_3 or Cl_2O. The mixture of ClO, Cl_2, He, and N_2 (or Cl_2, O_3/Cl_2O, He, and N_2 when the microwave discharge was off) flowed into the absorption cell, which was downstream of the flow tube.

Absorption Measurements. The concentrations of ClO, O_3, Cl_2O, and Cl_2 in the gas mixture were measured via UV absorption. The output of a D_2 lamp was passed through the combination of the absorption cell and the reactor and focused on to the entrance slit of a spectrograph. The 0.28 m spectrograph was equipped with a 1024 element diode array detector operated at ~230 K. The resolution of the spectrograph was ~1 nm (with a 100 μm entrance slit) and it covered the wavelength range of 220 to 370 nm. The total optical path length was measured to be 40.4 cm. The entire optical path was maintained at the temperature of the reactor.

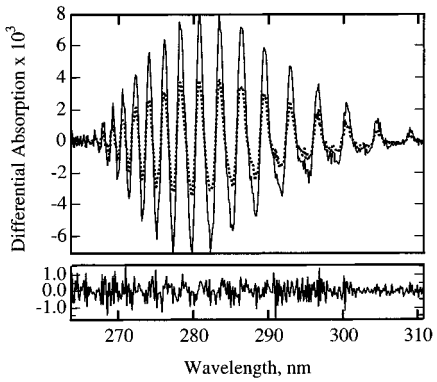

Figure 2. Top panel: Plots of the differential absorption versus wavelength for the reference spectrum of ClO (solid line) and the one measured in a kinetics experiment (dashed line). Bottom Panel: Residual from the subtraction of the two spectra in the above panel, with a suitable multiplication factor included. Clearly, there is no residual attributable to ClO.

The concentration of ClO was measured using the following procedure: (1) a spectrum with only N_2 flowing through the cell, I_0, was recorded. Then, the needed amounts of Cl_2 and O_3 or Cl_2O were added and another spectrum, I_1, was recorded. From these two spectra, the concentrations of Cl_2 and O_3 or Cl_2O were determined. (These concentrations were also determined from flow rate and pressure measurements and agreed well with the spectral determinations.) The microwave discharge was turned on to generate Cl atoms in the flow tube. The Cl atom concentration was variable but always much greater than that of ClO. The presence of excess Cl was evident from the visible emission (to the experimenter) due to the chemiluminescent Cl-recombination reaction. The excess Cl atoms reacted with O_3 or Cl_2O to generate ClO in the flow tube and ClO generation (and other possible reactions that affected its concentration) was complete in this region, i.e., before the flow entered the absorption cell. Then, another spectrum, I_2, was recorded. From the measured spectral differences between I_1 and I_2, the absorption due to ClO was obtained. The reference spectrum of ClO was subtracted from the difference spectrum ($I_2 - I_1$) until no structure attributable to ClO remained in the difference spectrum. One such example is shown in Figure 2, where the residual is clearly small and does not show the signature for ClO. The required absorption that had to be subtracted to get a residual of zero was converted to concentration by using the absorption at 265 nm and the known absorption cross section at this wavelength[16] ($\sigma_{ClO}^{265} = 5.29 \times 10^{-18}$ cm^2 molecule^{-1}). The ClO spectrum at this wavelength is nonstructured and its cross section here is independent of resolution and temperature.[10] The ClO reference spectrum at the temperature where k_1 was being determined and needed for the spectral subtraction was measured each day using the same setup, but with a high ClO concentration ([ClO] ~ 1×10^{14} molecule cm^{-3}). (Note that unlike our previous experiments involving ClO reactions, we did not have to correct for the number density gradients in the absorption cell.) The concentration of Cl_2O or O_3 was changed to vary the ClO concentration while keeping the Cl atom concentration nearly constant during the determination of a given value of k_1.

As discussed in our previous publications, we could detect ClO without interference from the other species that were present. The vibrational band structure of ClO was used to separate the absorption due to ClO from that due to other species in the absorption cell. This technique of locking onto the structure of ClO spectrum to determine the absorbance due to

ClO and then using the continuum part of ClO absorption to deduce the concentration has been successfully used in our laboratory in the past.[10,11] Also, as discussed in those papers, we measure the column abundance of ClO in the absorption cell. The ClO concentration was essentially the same over the entire length of the absorption cell. Small losses of ClO and their consequences to the concentration of ClO in the reactor are discussed later.

Once the concentration of ClO was measured, O atoms were generated via photolysis and their temporal profile was measured, as discussed below. After the temporal profile measurement, the concentration of ClO was again determined by measuring spectra I_2 and then I_1. The measured O atom temporal profiles were excluded from the determination of k_1 if the ClO concentrations measured before and after acquiring the temporal profile differed by more than 5%.

The photolysis beam was passed along the same path as the D_2 lamp beam. A movable mirror attached to a positive position mount was placed between the D_2 lamp and the absorption cell to introduce the photolysis laser beam into the reactor. The positive position mounts ensured that the photolysis laser beam traversed the same volume each time. A laser power meter was placed between the reactor and the spectrometer to measure the laser fluence. After acquiring the temporal profile, the mirror and the power meter were removed to pass the D_2 lamp beam through the absorption cell.

Reaction Cell and Atomic Resonance Fluorescence Detection System. The reaction cell for O atom detection was specially designed to reduce scattered light and, thus, improve the sensitivity for detection of O atoms. The cubic reaction cell was constructed from anodized aluminum with an internal volume of $\sim$250 cm^3 and an internal cross section of $\sim$20 cm^2. The O atom resonance lamp and solar blind photomultiplier tube (PMT) were mounted perpendicular to each other and orthogonal to the direction of the gas flow. Light traps were mounted opposite to the resonance lamp and PMT. The light traps measured 3.75 cm by 3.75 cm and consisted of an assembly of roughly 100 tightly stacked shiny stainless steel razor blades. The knife-edges of the blades faced the lamp and the PMT. This assembly appeared black because the knife-edges scatter the light sideways. A 3-cm long evacuated collar with two windows and a ring (internal radius of 0.5 cm) was located between the resonance lamp and reaction cell. This collar assembly, combined with a knife-edge machined into the reaction cell, improved the collimation of the resonance lamp radiation so that essentially all of it impinged on the light trap. Also, baffles were machined into the cell to minimize scattered light from the resonance lamp reaching the PMT. A CaF_2 window mounted in front of the PMT prevented Lyman-α radiation from reaching the detector.

The O atom detection limit in this reactor was measured to be better than 5×10^7 atom cm^{-3} for a 1s integration. This limit was determined by creating a known concentration of O atoms via photolysis of a known concentration of O_3 in N_2 with a known fluence of 308 nm from an excimer laser. This detection limit is at least a factor of 4 better than the detection sensitivities we obtained previously in cylindrical glass reactors.[14] The improved sensitivity made it easier to study reaction 1, a radical−radical reaction, under pseudo-first order conditions in O atoms while keeping the ClO radical concentrations relatively low (i.e., minimizing secondary chemistry of the ClO radicals) and in the presence of a large abundance of Cl_2, which absorbs the resonance lamp output and O atom fluorescence. The atomic resonance fluorescence lamp, detection system, and signal processing are basically the same as those used in previous works from this laboratory.

O Atom Generation. For measuring k_1, O atoms were produced by the pulsed photolysis of ClO at 308 nm (XeCl excimer laser; 20 ns pulse width):

$$\mathrm{ClO} \xrightarrow{h\nu(\lambda=308\ nm)} \mathrm{Cl} + \mathrm{O} \qquad (5)$$

The products of reaction 5 are assumed to be ground-state O and Cl atoms because there is insufficient energy to produce excited atoms. Also, for calculating the initial concentration of O atoms, $[O]_0$, we assume that the quantum yield for dissociation is unity since ClO does not fluoresce and the bands are quite broad. Note that the ratio of $[ClO]/[O]_0$ would only be larger if this quantum yield is not unity and does not affect the measured value of k_1. The photolysis laser fluence was varied over the range 4 to 18 mJ pulse^{-1} cm^{-2}. For a given series of experiments, where the ClO concentration was varied to obtain k_1, the laser fluence was kept constant. Thus, the fraction of ClO photolyzed remained the same and $[O]_0$ increased with increasing [ClO], i.e., $[ClO]/[O]_0$ was constant. The fraction of ClO photolyzed was usually between 0.2 and 0.8%, using a ClO absorption cross section at 308 nm of 3.0×10^{-19} cm^2 molecule^{-1}. (The XeCl laser beam is not monochromatic and has two peaks. The above cross section is the effective cross section for the wavelength distribution of the energy in the laser beam and the structured absorption of ClO reported by Trolier *et al.*[17]) Thus, pseudo-first-order conditions were ensured. In a few experiments, the laser fluence was decreased as the ClO concentration increased to keep the $[O]_0$ approximately constant. The laser repetition rate was varied between 7 to10 Hz, thus ensuring that the laser beam photolyzed a fresh gas mixture with each pulse.

The quantity of interest in calculating k_1 is the ClO concentration, $[ClO]_{Rx}$, in the volume where O atoms are detected. The second-order self-reactions,

$$\mathrm{ClO} + \mathrm{ClO} \rightarrow \mathrm{Cl_2} + \mathrm{O_2} \qquad (6a)$$

$$\rightarrow \mathrm{ClOO} + \mathrm{Cl} \qquad (6b)$$

$$\rightarrow \mathrm{OClO} + \mathrm{Cl} \qquad (6c)$$

deplete ClO along the absorption cell and the length of the reactor. The rate coefficient for these three reactions together is k_6 ($= k_{6a} + k_{6b} + k_{6c}$) $= 1.6 \times 10^{-14}$ cm^3 molecule^{-1} s^{-1} at 298 K. When the concentration of ClO is less than 5×10^{13} cm^{-3}, the average concentration along the length of the absorption cell, $[ClO]_{avg}$, lies within 5% of $[ClO]_{Rx}$, as discussed in our previous papers.[10,11] However, there is a difference between the position of O atom detection used here and the OH and IO detection region used in previous studies. In the present experiments, the O atoms were detected nearer to the end of the absorption cell (with respect to the flow direction), while the OH and IO detection regions in previous studies were in the middle of the absorption cell. In terms of the time available for ClO loss, however, the O atom detection zone was nearly at the midpoint between the entrance and exit of the absorption measurement region. This is because the cross section of the O atom detection cell was more than a factor of 4 larger than that of the glass absorption cell (see Figure 1) and the flow slowed substantially in the O atom detection region.

In an excess of Cl atoms, as in our present study, channel 6c does not lead to a net loss of ClO because OClO is converted

back to ClO,

$$Cl + OClO \rightarrow 2ClO \quad (7)$$

A small fraction (~10%) of the ClOO generated in reaction 6b is also converted to ClO via the reaction,

$$Cl + ClOO \rightarrow 2ClO \quad (8a)$$

$$Cl + ClOO \rightarrow Cl_2 + O_2 \quad (8b)$$

Thus, some of the ClO loss via reaction 6 does not lead to a net loss of ClO.

The wall loss of ClO in the glass flow tube is negligibly small. However, we have not previously used an aluminum cell and, thus, were unsure of the possible loss to this surface. Therefore, we checked for the wall loss of ClO by changing the flow rate of the gases through the reactor by a factor of ~3.5 at 298 K, ~2.5 at 231 K, and ~4 at 360 K. The measured values of k_1 were not affected as noted later.

When the concentration of ClO entering the absorption cell was 1×10^{14} cm^{-3}, its concentration is reduced by 20% by the time the flow exited the reactor due to reaction 6. The measured column average concentration was less than 10% lower than the concentration in the O atom detection region. At lower ClO concentrations, this difference is even smaller, as noted above. It should be noted that the depletion of ClO along the length of the apparatus was small and errors in k_1 introduced because of the correction to ClO concentration should be small. For example, if the error in the correction was 50% when the net ClO depletion was 20%, the maximum error in k_1 would be less than 10%.

At lower temperature, while reaction 6 slows down, ClO is lost via an additional pathway,

$$ClO + ClO + M \rightarrow Cl_2O_2 + M \quad (9)$$

For the residence times and pressure used here, the decomposition of Cl_2O_2 back to ClO can be neglected. At 250 K and 15 Torr, the difference between $[ClO]_{avg}$ and $[ClO]_{Rx}$ was ~15% for a residence time of 0.1 s. The residence time for a gas mixture in the absorption/photolysis/reaction cell varied between 0.06 and 0.1 s. This difference was smaller at lower pressures and shorter residence times. The calculated ClO concentrations in the O atom detection region explicitly accounted for the loss of ClO via reactions 6 and 9 at each given concentration of ClO. We assumed that the possible reaction of O atoms with Cl_2O_2 is slower than reaction 1 and did not correct k_1 for this possible loss process. The measured linear variation of k_1' with [ClO] supports this assumption.

The temperature of the gas flowing through the absorption/reaction cell was measured with two chromel−alumel thermocouples in direct contact with the gas flow. One thermocouple was located in the Pyrex absorption cell and the other in the reactor where the O atoms were detected. The thermocouples were inserted into the gas flow for the temperature measurement and withdrawn during the kinetic and absorption measurements. The gas temperatures measured in the two locations agreed to within 2 K under all our flow conditions. The temperature-controlled absorption cell protruded into the reactor (See Figure 1) such that there was very little difference in temperature between the absorption cell and the region where O atoms were detected.

Materials. Ozone was introduced to the flow tube by passing N_2 through a silica gel trap containing O_3. Cl_2O was prepared as described by Cady.[18] The largest impurity in the Cl_2O sample was Cl_2 (5%), which did not affect our measurements. The fraction of OClO in our sample of Cl_2O was below our detection sensitivity, <0.13%. Even if OClO were present, it would be converted to ClO via reaction with Cl. A mixture of Cl_2 (10%, electronic grade) in helium (99.98%) was used in the microwave discharge to generate Cl.

The concentration of Cl_2 in the reactor was determined from measured pressure and flow rates (using calibrated electronic mass flow meters). It agreed (within 5%) with the concentration measured via UV absorptions using the diode array spectrometer. In some experiments where N_2O photolysis was used to generate O atoms (see below), the concentration of N_2O was calculated from measured flow rates and pressure. Nitrogen was the carrier gas and its concentration was also obtained from measured flow rates and pressure.

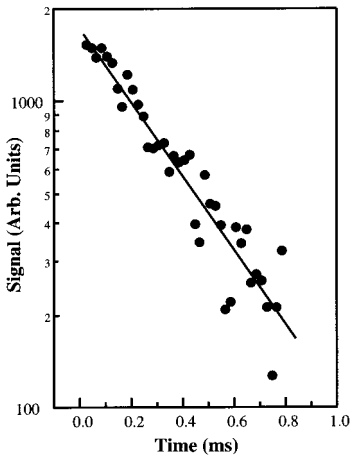

Figure 3. A temporal profile of O atoms recorded at 255 K with [ClO] = 6.3×10^{13} cm^{-3}, yielding an initial O atom concentration of ~1×10^{11} cm^{-3}. Data are shown every 20 μs and is the average of the adjacent 10 points. The data were collected with using 2 μs wide bins. The O atom signals in most experiments were much larger and the uncertainties in measured values of k_1' were smaller.

Results and Discussion

A representative O atom temporal profile measured in the presence of excess ClO is shown in Figure 3 and, as expected, it followed the equation for first-order kinetics:

$$\ln([O]_o/[O]_t) = (k_1[ClO] + k_d)t = k_1't \quad (10)$$

where k_d is the first-order rate coefficient for the loss of O atoms in the absence of ClO. The O atom temporal profiles were exponential for at least two lifetimes. A linear least-squares fit of the measured $\ln([O]_t)$ versus time to eq 10 yielded k_1'. The solid line in Figure 3 is the obtained fit. The temporal profiles of O atoms were recorded for at least 5, and usually 6 or 7, different ClO concentrations over the range (1 to 20) $\times 10^{13}$ molecule cm^{-3} to get one value of k_1. A plot of k_1' vs [ClO] yielded k_1 as the slope; one such plot is shown in Figure 4 where the line is a linear least-squares analysis of these data. The rate coefficient k_1 was measured at 10 different temperatures between 227 and 362 K. The obtained values, along with the experimental conditions used to derive them, are given in Table 1. The average value of the nine measurements at 298 K, weighted according to the noted errors in Table 1, yields k_1(298 K) of $(3.90 \pm 0.24) \times 10^{-11}$ cm^3 molecule^{-1} s^{-1}.

The intercepts in the plots of k_1' vs [ClO] could not be measured directly since we used ClO itself as the source of O

TABLE 1: Summary of Experimental Conditions and Results for O + ClO Kinetic Study

T (K)	pressure (Torr)	$[ClO]_{corr}$[a] (10^{13} cm^{-3})	$[O]_0$[b] (10^{11} cm^{-3})	flow velocity (cm s^{-1})	laser fluence (mJ cm^{-2} pulse^{-1})	k_1[c] (10^{-11} cm^3 molecule^{-1} s^{-1})
362	6.7	3.7−11.7	4−11	480	23	3.74 ±0.17
362	5.7	4.0−12.4	2−5	98−150	11−9	4.12 ± 0.11
343	5.5	2.5−10.6	1−4	490	8	3.80 ± 0.20
323	10.5	0.4−11.2	0.1−4	340−525	5−8	3.60 ± 0.13
317	8	3.3−11.0	1−6	460	7−12	4.00 ± 0.15[d]
298	10.5	3.2−13.6	3−11	280	20−17	4.14 ± 0.18
298	10.5	2.0−25.0	2−27	504	22	3.78 ± 0.17
298	6.7	2.5−6.9	0.2−10	500	31−2	3.50 ± 0.35
298	11.5	2.3−6.6	2−5	200	18	3.28 ± 0.47
298	11.8	1.8−6.0	0.3−1.2	240−300	4	3.97 ± 0.71
298	22	3.1−15.0	1−6	240	7−9	4.02 ± 0.24
298	8	4.0−13.0	1−3	150	5	3.43 ± 0.23
298	16.7	1.3−7.5	0.1−0.6	560	2	4.36 ± 0.28[d]
298	18.3	0.8−8.0	0.2−2	200	5	4.27 ± 0.24[d]
			average			3.90 ± 0.24
279	7.3	4.6−8.4	1−5	560	5−13	4.12 ± 0.35
279	11.0	3.2−12.6	1−3	300	6	4.20 ± 0.20
255	6.0	2.0−17.0	0.4−6	590	4−8	4.12 ± 0.14
237	7.8	2.0−12.0	1−4	730	11−7	4.46 ± 0.21
231	7.0	1.3−4.4	0.2−1	500	3	4.1 ± 0.37
231	9.0	1.7−9.2	1−8	770	13	4.1 ± 0.28
231	22.0	3.4−11.2	1−2	280	6	4.32 ± 0.44
227	8.0	1.8−9.1	1−3	780	12−7	4.43 ± 0.13[d]

[a] This is the concentration of ClO in the region where O atoms were detected. It was calculated by correcting the measured column ClO abundance for the loss of ClO in the absorption cell, as described in the text. [b] The concentrations of O atoms were calculated from the measured fluence and ClO concentrations and the known absorption cross section of ClO at 308 nm assuming the quantum yield for O atom production to be unity.[c] The quoted uncertainties are 1σ and were obtained from the fit of measured values of k_1' at various values of [ClO] to expression 10, as discussed in the text. [d] Cl_2O was used in place of O_3 to generate ClO via its reaction with Cl atoms.

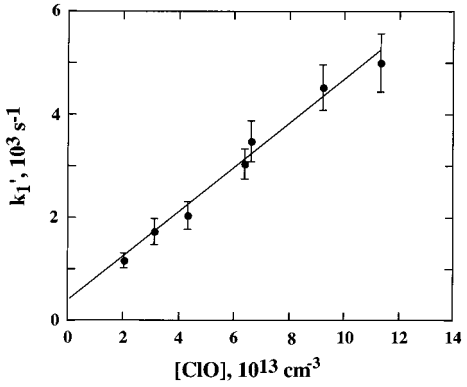

Figure 4. A plot of the measured values of k_1' vs [ClO] at 255 K. The error limits of the individual values of k_1' are 2σ from the fit of the O atom temporal profile to eq 10. The line is a linear least-squares fit to the equation: $k_1' = k_1 \times [ClO] + k_d$. The intercept is roughly consistent with the loss of O atoms due to pump out and reaction with Cl_2.

atoms. The fitted values were in the range 200 and 1000 s^{-1}. The O atom temporal profiles measured with Cl_2, O_3, and N_2 bath gas, the same gases as for making ClO but with the microwave discharge off (thus no ClO), could not be used to determine the intercept because the 308 nm radiation photolyzed Cl_2 and generated ClO. Therefore, the loss of O atoms in the absence of ClO was not routinely measured. This loss is determined by reaction with impurities, pump out from the detection zone, and its reaction with Cl_2:

$$O + Cl_2 \rightarrow ClO + Cl \qquad (11)$$

where $k_{11}(298) = 2.9 \times 10^{-14}$ cm^3 molecule^{-1} s^{-1}.[19] The values of the first-order rate coefficient for the removal of O atoms via pump out and reactions with impurities in the diluent gas were measured in a set of experiments where N_2O was photolyzed at 193 nm via the sequence:

$$N_2O + h\nu \rightarrow O(^1D) + NO \qquad (12)$$

followed by

$$O(^1D) + N_2 \rightarrow O(^3P) + N_2 \qquad (13)$$

We used flow rates that were similar to those used in measuring k_1 and a 193 nm excimer laser beam whose diameter was the same as that of the 308 nm beam used to photolyze ClO. The O atom loss rate constant due to pump out and reaction with impurities was measured to be 100 to 200 s^{-1}. This is similar to the values measured previously in our laboratory. Addition of $\sim 1 \times 10^{16}$ molecule cm^{-3} of Cl_2 increased the O atom loss to 600 ± 200 s^{-1}. Note that the photolysis of Cl_2 at 193 nm is very small due to its low absorption cross section ($< 1 \times 10^{-21}$ cm^2).[20] Therefore, it is clear that at least half of the O atoms are lost in the absence of ClO due to reaction with Cl_2. The uncertainties in the intercepts in the k_1' vs [ClO] were such that the rate coefficient measured with Cl_2 overlapped with the intercepts within the combined uncertainties. In any case, even if there was an error of 20−30% in the value k_d, it did not introduce a large uncertainty in k_1 because the values of k_1' measured in the presence of ClO were many thousands per second.

Figure 5 shows the measured values of k_1 in an Arrhenius form. A fit of the ln(k_1) vs 1/T to a straight line yielded the following value for the temperature dependence of k_1:

$$k_1(T) = (3.0 \pm 0.4) \times 10^{-11} \times \exp((75 \pm 40)/T) \text{ cm}^3 \text{ molecule}^{-1} \text{ s}^{-1}$$

where the uncertainty in E/R is the 2σ precision of the fit and uncertainty in A is twice the standard deviation in A defined as $\sigma_A = A\sigma_{\ln A}$.

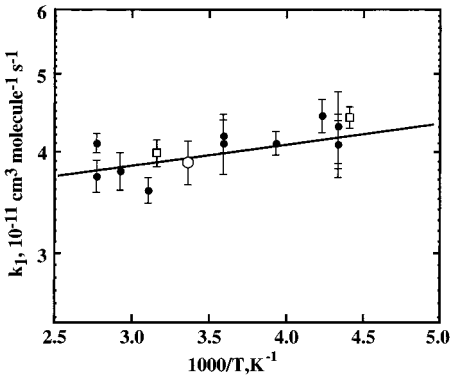

Figure 5. A plot of the measured values of k_1 (on a logarithmic scale) against the reciprocal of temperature. The line is a linear least-squares fit of $\ln(k_1)$ vs $1/T$ data. The values of k_1 measured using different ClO radical sources are shown as: circles (Cl + O_3) and squares (Cl + Cl_2O). The value shown at 298 K, open circle, is the average of nine measurements listed in Table 1 for this temperature.

Estimating the Uncertainty in k_1. A number of experimental parameters were varied in the determination of k_1 to minimize the influence of systematic errors. These parameters included: (1) total pressure and flow velocity (varied a factor of 3), (2) different ClO radical precursors (O_3 and Cl_2O), (3) altering the [ClO] over an order of magnitude, (4) changing the $[ClO]/[O]_o$ ratio by a factor of 4, and (5) varying the photolysis laser fluence a factor of 3. Variation of these parameters did not lead to significant changes in the value of k_1 (Table 1).

The most significant systematic uncertainty in the determination of k_1 lies in the value of $[ClO]_{Rx}$ used to calculate the rate coefficient. The uncertainty in the measured gas temperature, ±2 K, has only a small (<2%) affect on the ClO concentration and measured rate coefficient. The accuracy of $[ClO]_{Rx}$ is dependent on several factors each of which have associated uncertainties: the ClO absorption cross section, calculation of $[ClO]_{Rx}$ from $[ClO]_{avg}$, and the accuracy of the absorption measurements and spectral analysis. The use of the structured part of ClO spectrum to determine ClO absorption and extracting ClO concentration from the unstructured part of the spectrum leads to its better determination. As seen in Figure 2, the maxima in the residual was about 6% of the absorption due to ClO in the reactor. Therefore, we believe that we could measure ClO concentration with a precision better than about 6%. These factors are discussed elsewhere.[10,11] This spectral analysis method removes the common sources of error due to baseline stability and interference from nonstructured absorbers. When we combine this precision with the uncertainty in the absorption cross section of ClO in the unstructured part (~265 nm), about 5%, and the uncertainty in calculating the concentration of ClO in the O atom detection zone, we estimate the uncertainty in the ClO concentration in the O atom detection zone to be ~15% at the 95% confidence level.

Separate measurements were performed to test our determination of $[ClO]_{Rx}$. First, O atom signals were measured as a function of laser fluence (varied between 4 and 23 mJ $pulse^{-1}$ cm^{-2}) to confirm that it varied linearly with O atom concentration. Then, $[ClO]_{avg}$ was measured by absorption and the initial O atom signal from the photolysis of ClO, $[O]_{ClO}$, was measured. The microwave discharge was then turned off. The O_3 concentration was measured by absorption and the O atom signal from O_3 photolysis at 308 nm, $[O]_{O_3}$, was measured. All other conditions were held constant during this sequence. The ratio of the measured signals is proportional to the concentration of O_3 and ClO in the reaction zone and related by the equation:

$$\frac{[O]_{O_3}}{[O]_{ClO}} = \frac{[O_3]}{[ClO]} \times \frac{\sigma_{O_3}^{308}}{\sigma_{ClO}^{308}} \qquad (14)$$

With the O atom quantum yields for O_3 photolysis at 308 nm under our conditions (N_2 carrier gas) and of ClO photolysis at 308 nm both being unity, we could estimate $[ClO]_{Rx}$ from the measured signals and the $[O_3]$ along with the known absorption cross sections. The estimated value of [ClO] was within 15% of the value calculated from the measured ClO absorption using the diode array spectrometer and there was no systematic difference in the two values. This agreement serves as another verification of our determination of the ClO concentration. Such measurements could have been done for each temporal profile used to measure k_1. However, the fluctuations in the O atom detection sensitivity precluded such routine measurements.

The above tests and checks give us confidence in our determined values of $[ClO]_{Rx}$. Therefore, our measured rate coefficients are also uncertain by that amount. Including this estimated systematic uncertainty yields $k_1(298K) = (3.90 \pm 0.63) \times 10^{-11}$ cm^3 $molecule^{-1}$ s^{-1} and $k_1(T) = (3.0 \pm 0.7) \times 10^{-11} \exp[(75 \pm 40)/T]$ cm^3 $molecule^{-1}$ s^{-1}.

One of the possible complications in measuring k_1 is the potential interference through the reaction of ClO with $O_2(^1\Sigma)$, which can be a product of reaction 1.

$$O + ClO \rightarrow O_2(^1\Sigma) + Cl \qquad (15)$$

The subsequent reaction of $O_2(^1\Sigma)$ with ozone, if present, can regenerate O atoms. However, in our study, we used excess Cl and there was no possibility of O atom regeneration via the reaction of $O_2(^1\Sigma)$ with O_3 because of the absence of ozone. Another possible potential source of error was the loss of ClO on the walls of the aluminum reactor. As shown in Table 1, variation of the flow rate through the system by factors of roughly 3 did not vary the measured value of k_1. Given that the cross section of the aluminum cell is large and the flow rates were quite large, we should not expect a significant wall loss rate.

Comparison with Previous Measurements of k_1. Previous measurements of k_1 include mostly flow tube studies, with one notable exception being that by Nicovich et al.,[8] who used pressures of ~50 Torr in a pulsed photolysis system. Of the flow tube studies, only Leu[3] assumed a stoichiometric conversion of O_3 (or Cl_2O) to ClO and did not determine the ClO concentration by another method. Since the studies of Leu, it has become clear that neither O_3 nor Cl_2O is stoichiometrically converted to ClO in an excess of Cl atoms due to the reaction of Cl atoms with vibrationally excited ClO.[3,9,10,21] Recently, we have shown the difference between the expected and measured ClO in such a system to be substantial.[10] Therefore, the values of k_1 reported by Leu may be suspect. However, it should be noted that at the low concentrations of ClO used by Leu, the stoichiometry for conversion of O_3 to ClO is nearly 1-to-1and the rate constant may not be very far off the true value. Margitan[4] measured the concentration of ClO via UV absorption in the gas flow after the O atom temporal profiles were measured. He used the 277.5 nm band to quantify the ClO concentration. The cross section of this band, contrary to what Margitan noted, is quite sensitive to the resolution of the measurement. At the resolution of 0.3 to 0.5 nm (assuming it to be full width at half-maximum) used by Margitan, we estimate the ClO absorption at the peak to be ~6×10^{-18} cm^2 and

TABLE 2: The Values of k_1 at 298 K Reported in Previous Studies and Corrections to Some of Those Values

study	reported k (298 K)	modified k (298 K)	reason for the modification
Leu[3]	3.62	3.62	
Margitan[4]	4.2	3.5	adjusted for the resolution dependence of the absorption cross section at 277.5 nm
Schwab et al.[6]	3.5	3.5	
Zahniser and Kaufman[26]	4.3	4.13	adjusted for current recommendation for $k(Cl + O_3)$[22]
Ongstad and Birks[7]	3.76	3.63	adjusted for current recommendation for $k(O + NO_2)$[22]
Nicovich et al.[21]	3.7	3.7	
this work	3.90	3.90	
average		3.7 ± 0.4 (2σ)	

TABLE 3: Summary of k_1 Measurements (The values are those quoted by the authors; corrections to k_1(298 K) shown in Table 2 are not included here.)

reference	k(298K)[a]	f(298K)	A[a]	E/R (K)	$\Delta E/R$ (K)	T (K)	[ClO] measurement	technique[b,c]
Basco and Dogra[25]	1.2					298		Indirect[d]
Bemand et al.[24]	5.3 ± 0.8					298		DF −RF(O)
	5.7 ± 2.3					298		DF-MS(ClO)
Clyne and Nip[23]	5.2 ± 1.6		1.07 ± 0.30	224 ± 76		220−426	mass spec	DF−RF(O)
Zahniser and Kaufman[2]	4.35		2.12 ± 0.11	-75 ± 40		220−298		DF−RF(Cl)[e]
Leu[3]	3.62		5.0 ± 1.0	96 ± 20		236−422	indirect	DF−RF(O)
Margitan[4]	4.2		4.2 ± 0.8	0		241−298	UV absorption	DF-LFP−RF(O)
Ongstad and Birks[5]	3.5 ± 0.6					298	mass spec	DF−CL(O)[f]
Schwab et al.[6]	3.5		3.5 ± 0.5			252−347	LMR	DF-LMR(ClO) DF−RF(O)
Ongstad and Birks[7]	3.76		2.61 ± 0.60	-97 ± 64		220−387	mass spec	DF−CL(O)[f]
Nicovich et al.[21]	3.75		1.55 ± 0.33	-263 ± 60		231−367	indirect	LFP−RF(O)
this work[e]	3.9 ± 0.6		3.0 ± 0.8	-75 ± 40		227−362	UV absorption	DF/LFP−RF(O)
NASA[12]	3.8	1.2	3.0	−70	70		−	recommendation
CODATA[27]	5	1.26	5	0	250		−	recommendation
our recommendation	3.7	1.15	2.5	−110	25			

[a] Units of 10^{-11} cm^3 molecule^{-1} s^{-1}. [b] Abbreviations for various techniques used: DF, discharge flow; RF, resonance fluorescence; MS, mass spectrometry; LMR, laser magnetic resonance; CL, NO_2 chemiluminescence; LFP, laser flash photolysis. [c] The species monitored is in parentheses. [d] The rate coefficient was deduced from a mechanism that accounted for the changes in [ClO] in the flash photolysis of OClO and Cl_2O. [e] k_1 measured relative to $k(Cl + O_3)$. [f] Values include estimated systematic error.

definitely less than the 7.26×10^{-18} cm^2 used in his analysis. Thus, we estimate that his measured rate constants are high by ~20%, leading to a revised 298 K value of 3.5×10^{-11} cm^3 molecule^{-1} s^{-1}. Ongstad and Birks,[5,7] measured k_1 by directly determining the concentration of ClO and also by converting ClO to NO_2 via addition of NO and measuring the rate coefficient for the reaction of O with NO_2. We can change their measured value relative to the $O + NO_2$ reaction by using the currently accepted value.[22] Schwab et al. [6] measured k_1 in both excess ClO and O and their value at 298 K is in excellent agreement with ours. Zahniser and Kaufman,[2] measured k_1 relative to k_2. They argue that it is best to use the value of k_2 measured in their system. However, if we were to use the currently accepted value of k_2, their measured value of k_1 is reduced by only ~5%. The value of k_1(298 K) reported by Nicovich et al. [8] is in excellent agreement with our value. Table 2 lists the small changes to the previously reported values of k_1 because of the reasons noted above. All the previous values of k_1(298) (except the very old data of Bemand et al.[23,24] and Basco and Dogra[25]) agree with each other very well. The average of these values has a standard deviation of 10% at the 95% confidence level. Given that all these studies used very different methods and potentially had different systematic errors, we can confidently place an uncertainty factor of 1.15, in NASA/JPL notation, at the 1σ level. This is clearly one of the better-determined radical−radical reaction rate coefficients at 298 K.

A summary of the previous studies of the temperature dependence of k_1 is given in Table 3 and also shown in Figure 6. In this figure, we have not included the data of Bemand et al. and Leu; these are the two studies that reported a positive activation energy for this rate coefficient. Almost all the previous determinations of the temperature dependence of k_1 were carried out over limited ranges and by measuring at just a few temperatures. For example, Zahniser and Kaufman, Schwab et al., and Margitan measure k_1 at two temperatures other than 298 K. Leu measured k_1 at five temperatures and obtained a distinct positive temperature dependence. It is not clear as to why he saw such a dependence. The results of the more extensive studies of Ongstad and Birks, and of Nicovich et al.

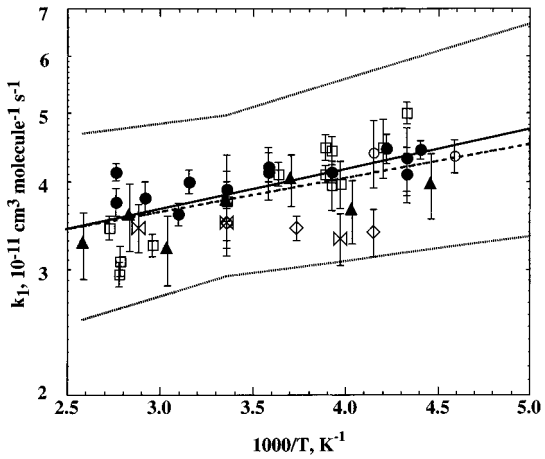

Figure 6. A comparison of our results (filled circles) with those discussed in the text. The data of Zahniser and Kaufman[2] (open circles) and of Margitan[4] (open diamond) have been corrected, as discussed in the text. The data of Schwab et al.,[6] (bow-tie) is that reported by the authors as the slopes of their k_1' vs [ClO] plots. The data of Nicovich et al.[21] (open squares) and Ongstad and Birks[7] (filled triangles) are also shown. The error bounds obtained from this combined data set, and discussed in the text, are shown for the 2σ level. The dashed line is the current recommendation of DeMore et al.[12]

can be combined with our results to deduce the temperature dependence of k_1:

$$k_1(T) = (2.39 \pm 0.42) \times 10^{-11} \times \exp[(130 \pm 50)/T]\ \text{cm}^3\ \text{molecule}^{-1}\ \text{s}^{-1}$$

where the error bars are at the 95% confidence level and $\sigma_A = A\sigma_{\ln A}$. Also, the preexponential factor has been slightly lowered to reproduce $k_1(298\ \text{K}) = 3.7 \times 10^{-11}\ \text{cm}^3\ \text{molecule}^{-1}\ \text{s}^{-1}$. These are the three studies that were carried out over extended temperature ranges, a necessity for quantification of small activation energies. These three studies also clearly observed that k_1 increased with decreasing temperature. We can also include the few points of Zahniser and Kaufman, Schwab et al., and Margitan (after correction for the cross section at 277.5 nm). Note that Margitan measured the concentration of ClO at 298 K and, hence, we do not have to account for the temperature dependence of the cross section of ClO at 277.5 nm. Figure 6 shows the data from these studies as an Arrhenius plot. Clearly, the collective data shows a negative temperature dependence and a linear least-squares analysis of $\ln(k_1)$ vs $1/T$ from all these studies yields

$$k_1(\text{T}) = (2.53 \pm 0.45) \times 10^{-11} \times \exp[(110 \pm 50)/\text{T}]\ \text{cm}^3\ \text{molecule}^{-1}\ \text{s}^{-1}$$

where the errors are the same as noted above.

Given that the studies of Nicovich et al.[8] were at pressures of tens of Torr, ours in the range of 5−20 Torr, and some of the previous flow tube studies in the range of 1−3 Torr, we can safely assume that k_1 is essentially independent of pressure, i.e., to within 20%. It appears that the higher pressure study of Nicovich et al. (∼50 Torr) yields slightly more negative activation energies than our results (6−20 Torr) and those from the discharge flow studies (1−2 Torr). These differences are small and there are sufficient systematic errors that we cannot make a strong correlation between pressure and measured activation energy. So, we do not attach much significance to this small difference. The activation energy derived from the combined data noted above should be appropriate for atmospheric calculations since the pressures and temperatures at which this reaction is important in the atmosphere has been covered in the laboratory. It would be interesting to measure this rate coefficient at higher pressures and, possibly, higher temperatures to see if the O−ClO intermediate can be quenched at higher pressure or if the reaction can proceed directly (i.e., without sampling the intermediate state) at higher temperatures. We suggest the following expression obtained by combining our results with those from selected previous studies for stratospheric calculations:

$$k_1(298\ \text{K}) = 3.7 \times 10^{-11}\ \text{cm}^3\ \text{molecule}^{-1}\ \text{s}^{-1};\ f(298) = 1.15$$

$$A = 2.4 \times 10^{-11}\ \text{cm}^3\ \text{molecule}^{-1}\ \text{s}^{-1};\quad E/R = 110\ \text{K};\ \Delta E/R = 25\ \text{K}$$

These error bounds, at the 95% confidence level, and the mean values are also shown in Figure 6.

Acknowledgment. This work was funded in part by NASA's Upper Atmospheric Research Program. L.G. thanks NASA for the Global Change Research Doctoral Fellowship.

References and Notes

(1) *Scientific Assessment of Ozone Depletion: 1998*; World Meteorological Organization, 1999.
(2) Zahniser, M. S.; Kaufman, F. *J. Chem. Phys.* **1977**, *66*, 3673−3681.
(3) Leu, M. T. *J. Phys. Chem.* **1984**, *88*, 1394−1398.
(4) Margitan, J. J. *J. Phys. Chem.* **1984**, *88*, 3638−3643.
(5) Ongstad, A. P.; Birks, J. W. *J. Chem. Phys.* **1984**, *81*, 3922−3930.
(6) Schwab, J. J.; Toohey, D. W.; Brune, W. H.; Anderson, J. G. *J. Geophys. Res.* **1984**, *89*, 9581−9587.
(7) Ongstad, A. P.; Birks, J. W. *J. Chem. Phys.* **1986**, *85*, 3359−3368.
(8) Nicovich, J. M.; Wine, P. H.; Ravishankara, A. R. *J. Chem. Phys.* **1988**, *89*, 5670−5679.
(9) Burkholder, J. B.; Hammer, P. D.; Howard, C. J.; Goldman, A. *J. Geophys. Res.* **1989**, *94*, 2225−2234.
(10) Kegley-Owen, C. S.; Gilles, M. K.; Burkholder, J. B.; Ravishankara, A. R. *J. Phys. Chem.* **1999**, *103*, 5040−5048.
(11) Turnipseed, A. A.; Gilles, M. K.; Burkholder, J. B.; Ravishankara, A. R. *J. Phys. Chem.* **1997**, *101*, 6667−6678.
(12) DeMore, W. B.; Sander, S. P.; Golden, D. M.; Hampson, R. F.; Kurylo, M. J.; Howard, C. J.; Ravishankara, A. R.; Kolb, C. E.; Molina, M. J. *Chemical Kinetics and Photochemical Data for Use in Stratospheric Modeling, Evaluation No. 12*; Jet Propulsion Laboratory, Pasadena, CA, 1997.
(13) Goldfarb, L. The photochemistry and kinetics of chlorine compounds important to stratospheric mid-latitude ozone destruction. Ph.D., University of Colorado, 1997.
(14) Goldfarb, L.; Harwood: M. H.; Burkholder, J. B.; Ravishankara, A. R. *J. Phys. Chem.* **1998**, *102*, 8556−8563; Goldfarb, L.; Schmoltner, A.-M.; Gilles, M. K.; Burkholder, J. B.; Ravishankara, A. R. *J. Phys. Chem.* **1997**, *101*, 6658−6666.
(15) Burkholder, J. B.; Wilson, R. R.; Gierczak, T.; Talukdar, R.; McKeen, S. A.; Orlando, J. J.; Vaghjiani, G. L.; Ravishankara, A. R. *J. Geophys. Res.* **1991**, *96*, 5025−5043; Burkholder, J. B.; Talukdar, R. K.; Ravishankara, A. R. *Geophys. Res. Lett.* **1994**, *21*, 585−588.
(16) Trolier, M.; Mauldin, R. L., III.; Ravishankara, A. R. *J. Phys. Chem.* **1990**, *94*, 4896−4907.
(17) Troe, J. *J. Chem. Phys.* **1977**, *66*, 4745−4757.
(18) Cady, G. H. *Inorgan. Synth.* **1957**, *5*, 156.
(19) Wine, P. H.; Nicovich, J. M.; Ravishankara, A. R. *J. Phys. Chem.* **1985**, *89*, 3914−3918.
(20) Hubinger, S.; Nee, J. B. *J. Photochem. Photobiol A: Chem.* **1995**, *86*, 1−7.
(21) Nicovich, J. M.; Wine, P. H.; Ravishankara, A. R. *J. Chem. Phys.* **1988**, *89*, 5670−5679.
(22) Sander, S. P.; Friedl, R. R.; DeMore, W. B.; Golden, D. M.; Kurylo, M. J.; Hampson, R. F.; Huie, R. E.; Moortgat, G. K.; Ravishankara, A. R.; Kolb, C. E.; Molina, M. J. *Chemical Kinetics and Photochemical Data for Use in Stratospheric Modeling, Evaluation No. 13*; Jet Propulsion Laboratory, Pasadena, CA, 2000.
(23) Clyne, M. A. A.; Nip, W. S. *J. Chem. Soc., Faraday Trans. 1* **1976**, *72*, 2211−2217.
(24) Bemand, P. P.; Clyne, M. A. A.; Watson, R. T. *J. Chem. Soc., Faraday Trans. 1* **1973**, *69*, 1356−1374.
(25) Basco, N.; Dogra, S. K. *Proc. R. Soc. A.* **1971**, *323*, 29; *323*, 401.
(26) Zahniser, M. S.; Kaufman, F.; Anderson, J. G. *Chem. Phys. Lett.* **1976**, *37*, 226−231.
(27) Atkinson, R.; Baulch, D. L.; Cox, R. A.; Hampson, R. F., Jr.; Kerr, J. A.; Rossi, M. J.; Troe, J. *J. Phys. Chem. Ref. Data* **1997**, *26*, 521.